The Journal of the Astronautical Sciences, Vol. 53, No. 4, October–December 2005, pp. 353–372

Low Energy Interplanetary Transfers Exploiting Invariant Manifolds of the Restricted Three-Body Problem[1]

Francesco Topputo,[2] Massimiliano Vasile,[3] and Franco Bernelli-Zazzera[4]

Abstract

In this paper, a technique for the analysis and the design of low-energy interplanetary transfers, exploiting the invariant manifolds of the restricted three-body problem, is presented. This approach decomposes the full four-body problem describing the dynamics of an interplanetary transfer between two planets, in two three-body problems each one having the Sun and one of the planets as primaries; then the transit orbits associated to the invariant manifolds of the Lyapunov orbits are generated for each Sun-planet system and linked by means of a Lambert's arc defined in an intermediate heliocentric two-body system.

The search for optimal transit orbits is performed by means of a dynamical Poincaré section of the manifolds. A merit function, defined on the Poincaré section, is used to optimally generate a transfer trajectory given the two sections of the manifolds. Due to the high multimodality of the resulting optimization problem, an evolutionary algorithm is used to find a first guess solution which is then refined, in a further step, using a gradient method. In this way all the parameters influencing the transfer are optimized by blending together dynamical system theory and optimization techniques.

The proposed patched conic-manifold method exploits the gravitational attractions of the two planets in order to change the two-body energy level of the spacecraft and to perform a ballistic capture and a ballistic repulsion. The effectiveness of this approach is demonstrated by a set of solutions found for transfers from Earth to Venus and to Mars.

Introduction

A class of future interplanetary missions would require the maximization of the payload mass without any particular restriction on the transfer time. For instance, the construction of a permanent base on Mars will require many preparatory missions aimed at delivering experiments and robotic devices on the planet. Moreover,

[1]Presented in part at the AAS/AIAA Space Flight Mechanics Meeting, Maui, Hawaii, February 2004 as paper AAS 04-245.

[2]Ph.D. Candidate, Aerospace Engineering Department, Politecnico di Milano, Italy, topputo@aero.polimi.it.
[3]Researcher, Aerospace Engineering Department, Politecnico di Milano, Italy, vasile@aero.polimi.it.
[4]Full Professor, Aerospace Engineering Department, Politecnico di Milano, Italy, bernelli@aero.polimi.it.

a manned journey to Mars could involve several cargo missions to carry the facilities necessary to allow human survival in hostile conditions. Such missions could be carried out by following low energy interplanetary trajectories through the libration points. On the other hand, as recently demonstrated by the designers of the Bepi Colombo mission [1], a gravitational capture can be used to avoid a single point failure of a classical chemical orbit insertion burn typical of a hyperbolic approach. These goals can be achieved all together by extending the classical two-body model used to define the interplanetary transfer trajectories.

When an interplanetary trajectory is designed by the patching conic technique, indeed, several two-body problems are solved at a time and different conic arcs are linked together in order to define the whole path. By this technique the transfer problem can be formulated analytically and this description fits well with the further optimization processes. If the problem is well-posed and the solution exists, a transfer that minimizes a certain function, usually the total cost (Δv), in order to maximize the payload mass or to reduce the launch mass, can be found. The resulting trajectory, due to the discontinuities involved with its definition, is intrinsically forced to high energy levels making the patched-conic path a good first guess solution in the further refinement processes.

If a low energy level is required, as for the ballistic capture, the effects of more than one gravitational attraction acting on the spacecraft can be appreciated. Low energy trajectories exploiting such a feature have been proven to provide a reduced Δv cost [2]. However, within an n-body problem, the definition of the orbits is not a trivial task since the integrability of the system is lost and the analyticity of the solution no longer exists. In particular, the conservation of the angular momentum vanishes and so the orbital parameters, useful for the description of the two-body motion, are no longer defined. Moreover, even if n-body problems are governed by Newtonian dynamics, they turn out to be chaotic in nature and make trajectory design a challenging task.

The easiest extension of the two-body model is represented by the circular restricted three-body problem (CR3BP). This problem has only one integral of motion (the Jacobi constant) meaning that the lost information has to be replaced using the dynamical knowledge of the phase space. Hence, the equilibrium points L_1 and L_2, the periodic orbits around them and the invariant manifolds associated both to the libration points and to the periodic orbits should be used as dynamical "tools" in order to assure preliminary information to the design.

In the past, much attention has been paid to the description of the restricted three-body problem (R3BP) dynamics, especially in the neighborhood of the equilibrium points. Llibre et al. [3] analyzed the behavior of the invariant manifolds associated to the periodic orbits around L_2. They established the existence of separatrices for the states of motion demonstrating the relevance of the dynamical system theory for qualitative analyses. The same theory was used by Howell et al. [4] to formulate a general method for the trajectory design of libration point missions in the Sun-Earth system. This technique is based on the injection of the spacecraft on the stable manifold associated to the final periodic orbit around L_1 or L_2.

More recently, the works of Koon et al. [5–7] evidenced the importance of the invariant manifolds associated with the periodic orbits around libration points. These tubes, due to their property described in Llibre et al., separate different orbits in the phase space: those transiting through the forbidden region and those

remaining forever in the exterior or in the regions around the two primaries. Hence, if an intersection between the manifolds of two different systems occurs in the configuration space, a Δv maneuver performs the intersection in the whole phase space and a low energy transfer between two bodies could be accomplished with the coupled three-body problems approximation. This invariant manifolds approach allowed to explain the dynamics behind the Weak Stability Boundary (WSB) transfers to the Moon [2, 6] and led to the formulation of a general technique to obtain low energy transfers in the solar system [7]. The invariant manifolds technique represents a smart solution to overcome the difficulty of designing transfers in the four-body problem but it requires an intersection of the manifolds in the configuration space for the definition of the final trajectory. This makes such a method only suitable for transfers, as between two outer planets or two moons around a giant planet, where the physical constants and the orbital parameters allow the required intersection. Unfortunately, such interplanetary transfers (e.g., Jupiter-Saturn) entail very long times of flight making these solutions of questionable practical use [5].

The present study deals with the possibility to further develop the invariant manifolds technique in order to design interplanetary transfers among inner planets even if an intersection between the manifolds does not occur. Venus, Mars, and Earth have been considered since Mercury, due to the high value of its orbital eccentricity, does not match the hypothesis of the CR3BP. Analyzing the profile of the two-body energy associated to the manifolds of the points, a hypothesis has been formulated on the conservation, after a finite period, of such two-body energy. Hence, an additional two-body problem has been added to the two R3BPs and the non-intersecting manifolds have been linked by using an intermediate conic or thrust arc. The full four-body model is divided into a first three-body problem (Sun-Earth-spacecraft), an intermediate two-body problem (Sun-spacecraft) and a final three-body problem (Sun-target planet-spacecraft). The proposed patching conic-manifolds method exploits the two gravitational attractions of the planets to change the energy level of the spacecraft and to perform a ballistic capture and a ballistic repulsion.

A computational algorithm is presented to design such transfers: first, a merit function is associated to the Poincaré sections of the manifolds, with the surface of section that is free to move to find a suitable configuration of the system; then, an optimization step minimizes the total cost for the transfer between two circular orbits, one around the Earth and the other around the target planet. The solutions found show that cheaper transfers, if compared to the Hohmann solutions linking the same departure and arrival orbits, could be accomplished with the developed technique. Since the results depend on the mass parameter, characterizing the R3BP considered, a preliminary description of such a model is given.

Dynamics of the R3BP

Equations of Motion

The equations describing the planar motion of a particle (here called spacecraft) under the gravitational attractions of two primaries (here called Sun and planet) are written in a synodic system. This rotating system has the origin in the Sun-planet center of mass and the x-axis defined by the Sun-planet line with the planet on the positive direction. Normalizing the distance between the primaries to one, their

angular velocity to one (the period is equal to 2π), indicating with m_P the mass of the planet and m_S the mass of the Sun and introducing the mass parameter of the problem as

$$\mu = \frac{m_P}{m_S + m_P} \tag{1}$$

the equations of motion can be written in the second order Lagrangian form as [8]

$$\begin{aligned} \ddot{x} - 2\dot{y} &= \Omega_x \\ \ddot{y} + 2\dot{x} &= \Omega_y \end{aligned} \tag{2}$$

where the subscripts denote the partial derivatives of

$$\Omega(x, y) = \frac{1}{2}(x^2 + y^2) + \frac{1-\mu}{r_1} + \frac{\mu}{r_2} + \frac{1}{2}\mu(1-\mu) \tag{3}$$

with respect to the coordinates of the spacecraft (x, y). The two radial distances in equation (3) are

$$\begin{aligned} r_1 &= \sqrt{(x+\mu)^2 + y^2} \\ r_2 &= \sqrt{(x-1+\mu)^2 + y^2} \end{aligned} \tag{4}$$

The system has a first integral of motion, called the Jacobi integral, which is given by

$$C(x, y, \dot{x}, \dot{y}) = 2\Omega(x, y) - (\dot{x}^2 + \dot{y}^2) \tag{5}$$

and represents a three-dimensional manifold for the states of the problem within the four-dimensional phase space. Once a set of initial conditions is given, the Jacobi integral defines some forbidden and allowed regions bounded by zero velocity or Hill's curves. Such curves, defined by equation (5) with the kinetic term set to zero, are useful for a qualitative analysis of the motion giving a rough depiction of the energy level. The energy of the spacecraft and the Jacobi constant are related by

$$C = -2E \tag{6}$$

which states that a high value of C is associated with a low energy of the spacecraft. For a low value of the energy the spacecraft is bounded to orbit around one of the two primaries. If the energy is increased the allowed regions of motion enlarge and the spacecraft is free to leave one of the primaries (Fig. 1).

Libration Points

The fixed points of the system are defined as the singular points of the Jacobi constant [8]

$$C_x = C_y = C_x = C_y = 0 \tag{7}$$

which means, from equation (5), that

$$\Omega_x = \Omega_y = \dot{x} = \dot{y} = 0 \tag{8}$$

and by equation (2) one can easily find that in such points the dynamics reduces to

$$\ddot{x} = \ddot{y} = 0 \tag{9}$$

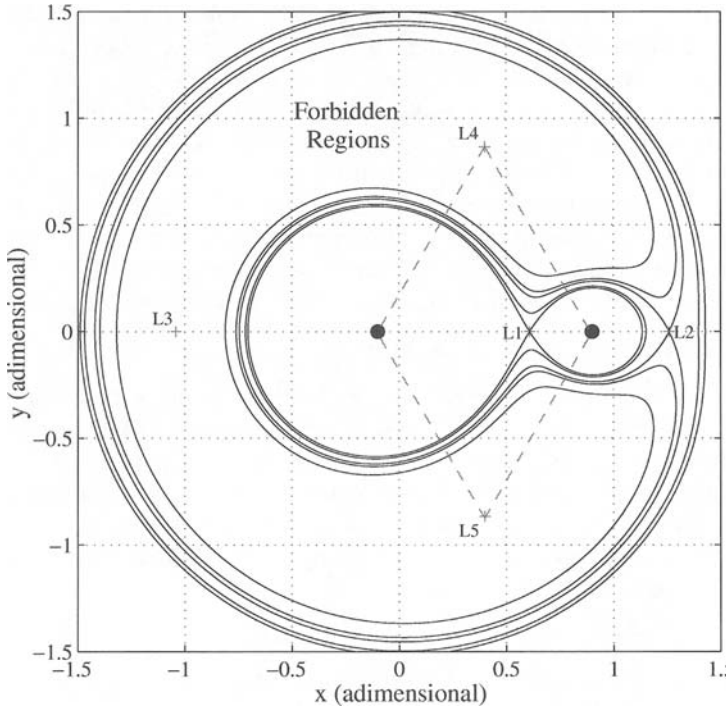

FIG. 1. Libration Points and Hill's Curves for Several Values of C with $\mu = 0.1$.

or both the velocities and the accelerations, relative to the synodic frame, are equal to zero. Hence, the singular points of the 3-D submanifold $C = constant$ are equilibrium points for the dynamical system.

The five Lagrangian, or libration, points, shown in Fig. 1, represent also some zero-dimensional manifolds in the phase space: three, called L_1, L_2, and L_3, are collinear with the primaries; two, L_4 and L_5, are at the vertex of two equilateral triangles with the primaries. The linearized dynamics around the three collinear points is always like the product of a saddle times a center, so these points are unstable; on the contrary, the stability of the triangular points depends on the mass parameter of the system [8].

The present study deals with the possibility to obtain free arcs of transfer exploiting the nature of the libration points. This goal can be achieved only considering L_1 and L_2, since L_3 has a "slow dynamics and a mild instability" [9] while triangular points L_4 and L_5 are always stable for any Sun-planet-spacecraft problems in the solar system; therefore they are not suitable for the design of transfers among planets. Furthermore low energy levels, or high values of the Jacobi constant in equation (6), are associated with L_1 and L_2. This means that already for low energy levels, Hill's curves open at L_1 and L_2 allowing the motion of the spacecraft outside the forbidden regions.

While the position of the triangular points is trivial, the location of the collinear points can be found by solving fifth-order polynomials derived by the equation (8). These equations give the distance from the planet (smallest primary) to both L_1 and L_2. They can be solved numerically by Newton's method using, for small values of

μ, the value $(\mu/3)^{1/3}$ as a good starting point [10]. Table 1 shows the mass parameter and the dimensionless x-coordinate of L_1 and L_2 for the problems discussed in this paper.

Although both L_1 and L_2 represent unstable equilibria, some infinitesimal Lyapunov orbits, lying in the x-y plane, can be obtained by the linearized equations of motion with initial conditions that cancel the stable and unstable parts. They can be continued, under the whole dynamics, to finite size periodic orbits. Since these periodic solutions orbit an unstable equilibrium point, there are some invariant manifolds associated with them. These 2-D tubes have been employed in this study to define the low energy trajectories that approach or depart from the planet.

Invariant Manifolds of the Lyapunov Orbits

The method used to compute the manifolds of the orbits is based on the linear approximation of the flow mapping around a periodic orbit. Thus, once the monodromy matrix M associated with a periodic orbit has been obtained, the manifolds are computed by propagating the flow along the directions associated with the Floquet multipliers of that orbit. In particular, since the monodromy matrix represents the first-order approximation for the mapping of $\mathbf{x}_0$ into a point $\mathbf{x}$ on a generic surface of section

$$\mathbf{x} \mapsto \mathbf{x}_0 + M(\mathbf{x} - \mathbf{x}_0) \tag{10}$$

its eigenvectors give the direction of the 1-D manifolds of the $\mathbf{x}_0$ point. Hence, its associated stable manifold can be obtained by propagating backward the initial condition

$$\mathbf{x}_{0,S} = \mathbf{x}_0 \pm \varepsilon \mathbf{v}_S \tag{11}$$

where $\mathbf{v}_S$ is the eigenvector associated with the stable eigenvalue of the monodromy matrix evaluated in $\mathbf{x}_0$.

In the same way, the unstable manifold associated to that point can be achieved by forward integration with initial condition taken in the direction of the unstable eigenvector. The invariant manifolds tube can be obtained by repeating this process for each point of the orbit.

The perturbation ε represents the distance, in the direction of the eigenvectors, between the orbit and the initial condition taken for the integration. It is obvious that the smaller the value of ε the better the approximation of the manifold is that this first-order method can supply. The value of ε is typically bounded between 10^{-4} and 10^{-6}.

It is important to observe that, since the Jacobi constant is a three-dimensional surface, the manifolds of the orbits are separatrices and they split different regimes

TABLE 1. Mass parameter and location of L_1 and L_2 in the Sun-Planet problems faced in this study. The mass parameter of the Sun-Earth system takes into account the presence of the Moon.

System	$\mu \cdot 10^6$	L_1	L_2
S-Venus	2.4510	0.9906782	1.0093750
S-Earth	3.0359	0.9899909	1.0100701
S-Mars	0.3233	0.9952484	1.0047659

of motion. This means that orbits lying on the manifolds are asymptotic trajectories and wind to or from the periodic orbits; those starting inside the tubes, flowing under the dynamical system, will continue to remain in that tube. These trajectories are called transit orbits because they are the only ones able to go through the small allowed region and to approach the planet for a given energy value (Fig. 2). Recently, the behavior of these orbits under the influence of perturbing forces has been investigated by Yamato and Spencer [11].

The present work aims at using the invariant manifolds theory as additional information for the trajectory design within the R3BP. This means that, once an energy level has been fixed and a periodic orbit around the libration point has been computed, the associated transit orbits are the candidate trajectories useful to a low energy transfer between two bodies.

When a transit orbit is built and propagated using equations (2) in the synodic reference frame, it can first be translated in the planar sidereal coordinate system (planets in planar and circular orbits) and then, using an analytical ephemeris model, in the 3-D space by the transformation

$$\mathbf{X}^{\text{abs}} = R\mathbf{X}^{\text{sid}} \tag{12}$$

taking into account the real eccentricity and inclination of planetary orbits. The first term in (12) represents the trajectory in the 3-D absolute Sun-centered reference frame, $R = R(i, \Omega, \omega, \theta)$ is the rotation matrix and $\mathbf{X}^{\text{sid}}$ is the trajectory in the sidereal system

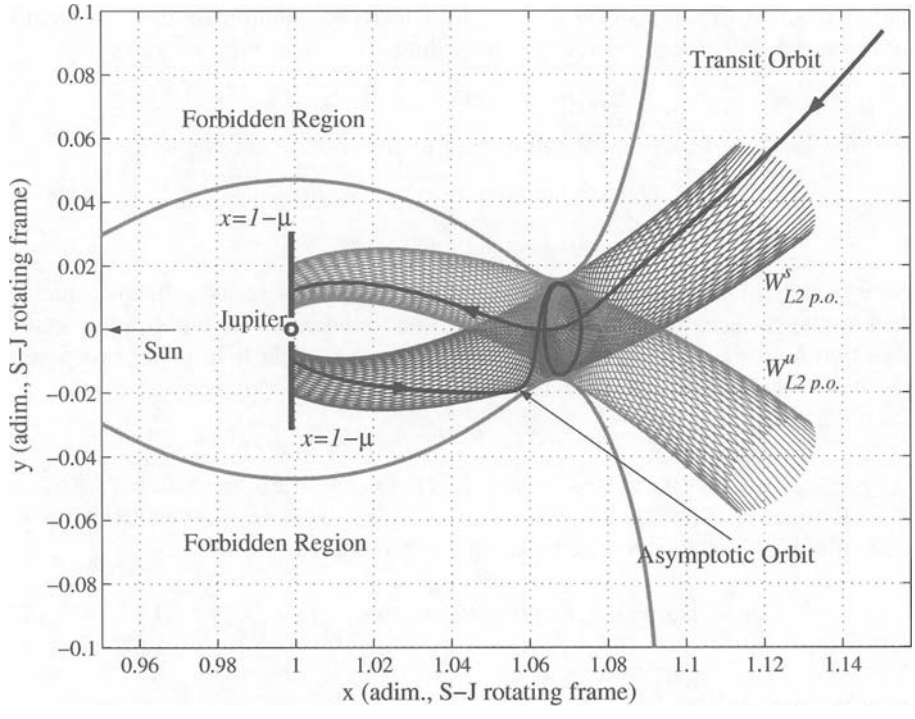

FIG. 2. Invariant Manifolds Associated with a Lyapunov, Transit, and Asymptotic Orbits near the Sun-Jupiter L_2.

$$\mathbf{X}^{\text{sid}} = \{x^{\text{sid}}, y^{\text{sid}}, 0\}^{\text{T}} \tag{13}$$

Repeating the same process for the velocities, it is also possible to obtain the velocity vector in the absolute Sun-centered reference frame.

The Design Approach

Intersecting the Manifolds

The manifolds of different Sun-planet systems are computed in the synodic frames and then translated in the Sun-centered sideral frame because this system represents a homogeneous environment when looking for an intersection between the manifolds. The transformation from the synodic to the sideral frame introduces a time variable or a phase angle, here called θ, between the planets.

The manifolds associated with a Lyapunov orbit can be computed given the semi-amplitude of the orbit A_x and ε, the parameters introduced in the previous section. If θ is the angular location of a surface of section, the three variables ε, A_x, and θ uniquely define a configuration for the manifold. Without any loss of generality, the starting planet, generically called P_a, is taken aligned with the x-axis and its unstable manifold develops until the angular coordinate is $\theta = \theta_a$. The stable manifold, taken from the second R3BP, develops until $\theta = \theta_b$, so the arrival planet, called P_b, has an angular position equal to $\theta_a + \theta_b$ (Fig. 3). Working with polar coordinates and using θ as a parameter, the surface of section can be easily shifted by varying its value.

By giving the following set of six variables $[\varepsilon_a, A_{x,a}, \theta_a, \varepsilon_b, A_{x,b}, \theta_b]$ the two manifolds shown in Fig. 3 can be computed. The representation of the two section curves on the Poincaré surface is given by the two curves (Fig. 4)

$$\gamma_a(r_a, \dot{r}_a) \quad \text{and} \quad \gamma_b(r_b, \dot{r}_b) \tag{14}$$

On the surface of section the following function can be defined as

$$D(r_a, \dot{r}_a, r_b, \dot{r}_b) = \sqrt{\alpha(r_a - r_b)^2 + \beta(\dot{r}_a - \dot{r}_b)^2} \quad \begin{matrix}(r_a, \dot{r}_a) \in \gamma_a \\ (r_b, \dot{r}_b) \in \gamma_b\end{matrix} \tag{15}$$

where α and β are two weighting factors. Such a parameter is a distance metric, taken on the surface of section, that can be used to indicate how close in the section space two points belonging to the manifolds are. It is clear that, given two points, D is also a function of the variables introduced so far

$$D = D(\varepsilon_a, A_{x,a}, \theta_a, \varepsilon_b, A_{x,b}, \theta_b, \alpha, \beta) \tag{16}$$

Given the two section curves γ_a and γ_b, enclosing an infinite number of transit orbits, the metric D selects the two points, $A \in \gamma_a$ and $B \in \gamma_b$, which correspond to the minimum distance metric between the two curves

$$A, B = \left\{ (r, \dot{r}) \in \mathcal{R}^2 : D(A, B) = \min_{\substack{(r_a, \dot{r}_a) \in \gamma_a \\ (r_b, \dot{r}_b) \in \gamma_b}} D(r_a, \dot{r}_a, r_b, \dot{r}_b) \right\} \tag{17}$$

Departure and Arrival Legs

The two points A and B selected by equation (17) correspond to two asymptotic orbits wrapping onto the two sources Lyapunov orbits defined by $A_{x,a}$ and $A_{x,b}$. If

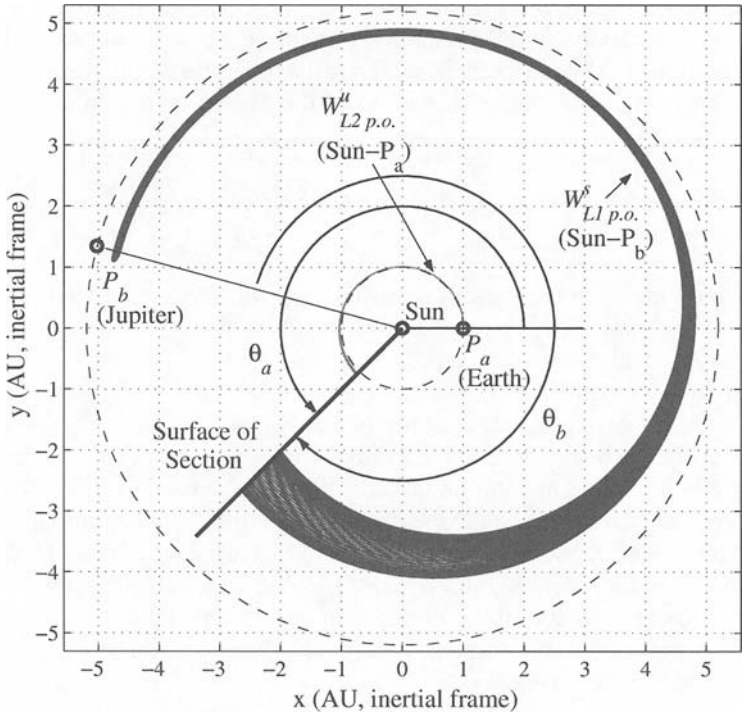

FIG. 3. Geometry of the Invariant Manifolds in the Sideral Plane for the Earth-Jupiter Case.

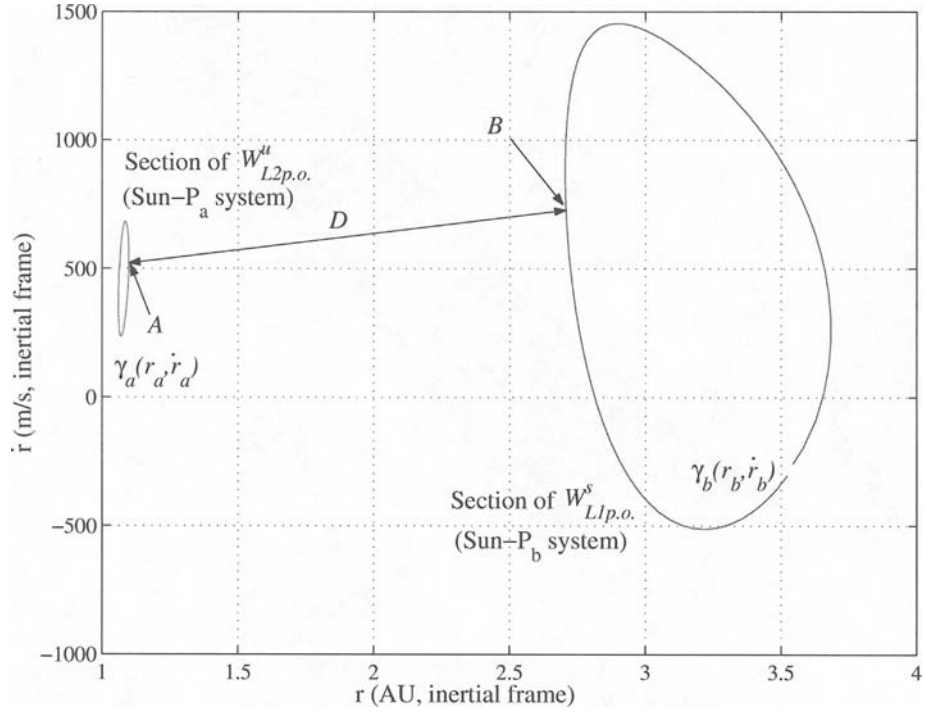

FIG. 4. Poincaré Section of the Two Manifolds in Fig. 3 and Geometric Representation of the Parameter *D*.

these two conditions are used to define the departure and arrival legs, a link between the two libration points is obtained instead of a link between the two planets. The two transit orbits, departure and arrival legs of the whole transfer path, are computed by propagating the perturbations of the two points A and B

$$A \pm \delta A \quad \text{and} \quad B \pm \delta B \tag{18}$$

where δA and δB are assumed arbitrary small, for instance equal to

$$\delta A = \omega\{(r_{a,\max} - r_{a,\min})\,(\dot{r}_{a,\max} - \dot{r}_{a,\min})\} \tag{19}$$

and the same for δB. In the present paper the perturbation ω has been taken equal to 0.01. The sign ambiguity in equation (18) is solved with the imposition that both points must lie inside the two curves.

Propagations, forward for the arrival leg and backward for the departure one, stop when the closest approach with the planet is reached. Figure 5 shows the arrival transit orbit corresponding to the example in Figs. 3 and 4. In systems with intersecting manifolds the method described so far can be used to find a low energy transfer between two bodies; such property can be exploited when moving between two outer planets or between two moons around a giant planet. Nevertheless, when inner planets are considered (Earth, Mars, and Venus assumed in this work) the manifolds do not intersect or their intersection occurs very seldom. Since this work aims to find low energy transfers between inner planets, an intermediate arc must be added to match the two legs.

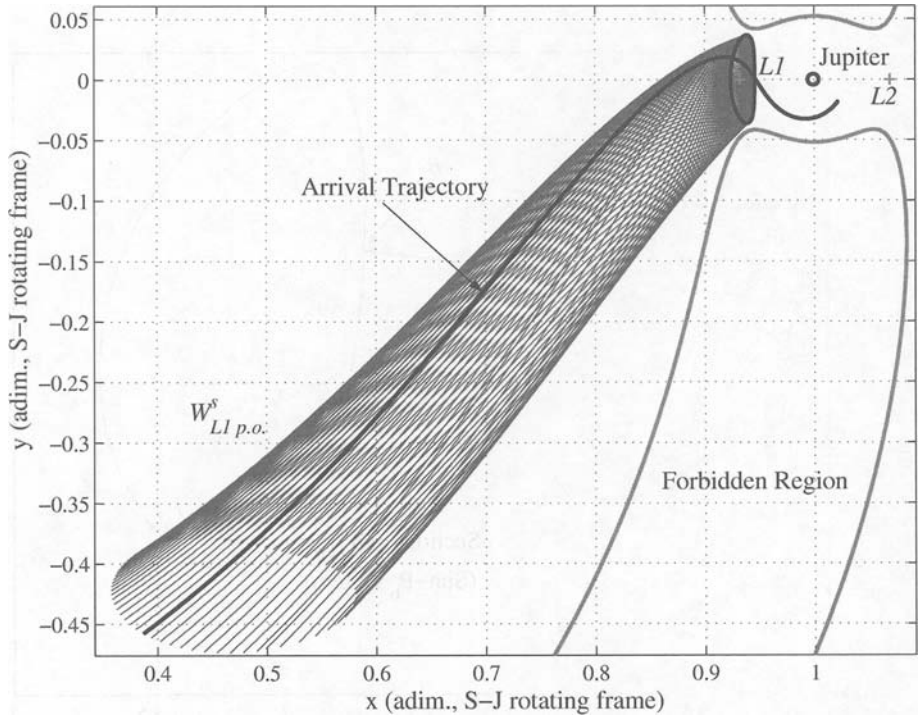

FIG. 5. Arrival Transit Orbit in the Synodic System.

Link Hypothesis

As stated above, a low energy transfer between two celestial bodies could be obtained by intersecting the manifolds of the two R3BPs considered so far. When the manifolds intersect in the configuration space but not in the phase space, a single Δv maneuver is sufficient to link the two transit orbits. Unfortunately, the R3BPs involved in this study, due to their small mass parameters (Table 1), do not allow the manifolds to develop far enough in order to approach each other; hence in this case the manifolds do not intersect even in the configuration space. This holds in a simple model considering circular and coplanar orbits. In more refined models, contemplating the full solar system dynamics, a closer approach or even an intersection, after hundreds of years, may occur. If no intersection occurs both in the configuration and phase space, the existing technique [6, 7] does not apply and a further development is required to find solutions of practical interest.

The four-body problem, characterizing such low energy transfers, has been approached by examining the behavior of the transit orbits far from both primaries. For instance, let us consider the external leg of the L_2 unstable manifold ($W^U_{L_2}$) in the Sun-Earth system. This manifold, indeed, is close in the phase space to the low energy transit orbits, escaping from the Earth, associated to small size Lyapunov orbits. If ($W^U_{L_2}$) is integrated for a long time, it could be noticed that, after an initial evolution, the trajectory becomes invariant and quasi-periodic. This suggests that, in general, if no other actions are considered, in systems with a low mass parameter and far from the smallest primary a spacecraft is only subject to the gravitational attraction of the largest primary. This statement can be verified by analyzing the Sun-spacecraft two-body energy associated to that manifold without considering the presence of the Earth. It is well known, indeed, that in the two-body problem (2BP) the energy remains constant, therefore for any point of ($W^U_{L_2}$) this quantity can be calculated through

$$E = \frac{1}{2}v^2 - \frac{k_S}{r} \tag{20}$$

where r and v are respectively the modulus of the position and the velocity vectors, both expressed in the absolute system and k_S is the gravitational constant of the Sun.

As can be seen in Fig. 6, the two-body energy $E = E(t)$, after an initial growth, when the spacecraft is close to the Earth, remains almost constant and the motion of the spacecraft is mainly governed by the Sun. This means that flowing on a transit orbit corresponds, in the two-body representation of the dynamics, to an energy change, provided by the planets' gravitational fields, which can be either a propulsive effect, at departure, or a braking effect, at arrival. These effects can be seen in the fast growth of E in Fig. 6.

On the other hand, when the spacecraft is far from both planets, the energy associated with the Sun-spacecraft 2BP stabilizes about a constant value and the end point of the two transit orbits, shown in Fig. 7, can be considered subject only to the gravitational attraction of the Sun and linked with a conic arc, solution of a Lambert's problem.

Therefore the existing technique in [6, 7] has been extended to treat cases in which no intersection between the manifolds can be found. The full four-body problem is decomposed as follows:

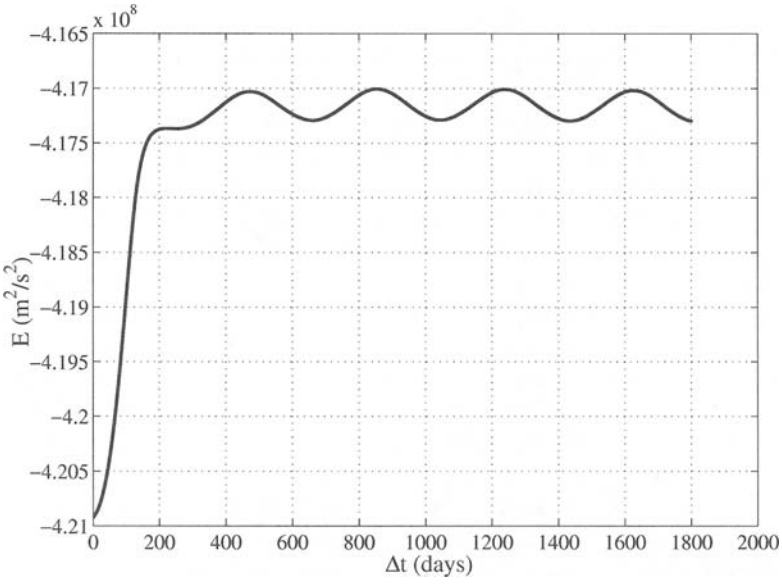

FIG. 6. Two-Body Energy Associated with W_{L2}^{U} (Sun-Earth Systems) Integrated for Five Years.

- an initial R3BP with the Sun and the departure planet as primaries. The unstable manifolds associated to the periodic orbits around L_1 or L_2 are computed in this system together with their transit orbits;
- an intermediate Sun-spacecraft 2BP in which a conic arc links the extremes (or terminal points) of the two transit orbits;
- a final R3BP the Sun and the arrival planet as primaries. The stable manifolds of periodic orbits around L_1 or L_2 and the transit orbits, ballistic captured trajectories, are computed in this second frame.

Two intermediate deep space maneuvers, leading to a multi-burn transfer, are then required to realize the link in the phase space between the conic arc and the stable and unstable transit orbits. The total cost associated with the conic link can be tuned either by changing the width of the departure and arrival periodic orbits, with a consequent change of the energy associated to the transit orbits, or by varying the time of the Lambert's arc.

The Patched Conic-Manifold Method

As shown in Fig. 7, the departure and arrival legs are translated into a sideral heliocentric reference frame by introducing a time variable and the real ephemeris of the planets. Since the planar R3BP has been assumed to derive the transit orbits, these are on the planets orbital planes. If T_S is the departure epoch and Δt_L is the time interval of the Lambert's arc, the variable vector

$$\mathbf{x} = \{\varepsilon_a, A_{x,a}, \theta_a, \varepsilon_b, A_{x,b}, \theta_b, \alpha, \beta, T_S, \Delta t_L\} \tag{21}$$

uniquely defines a transfer trajectory. The vector $\mathbf{x}$ takes into account the parameters used to describe the two transit orbits (equation (16)) and those needed to compute the Lambert's arc. The total cost for a *patched conic-manifold transfer* is

$$\Delta v(x) = \Delta v_S + \Delta v_1 + \Delta v_2 + \Delta v_E \tag{22}$$

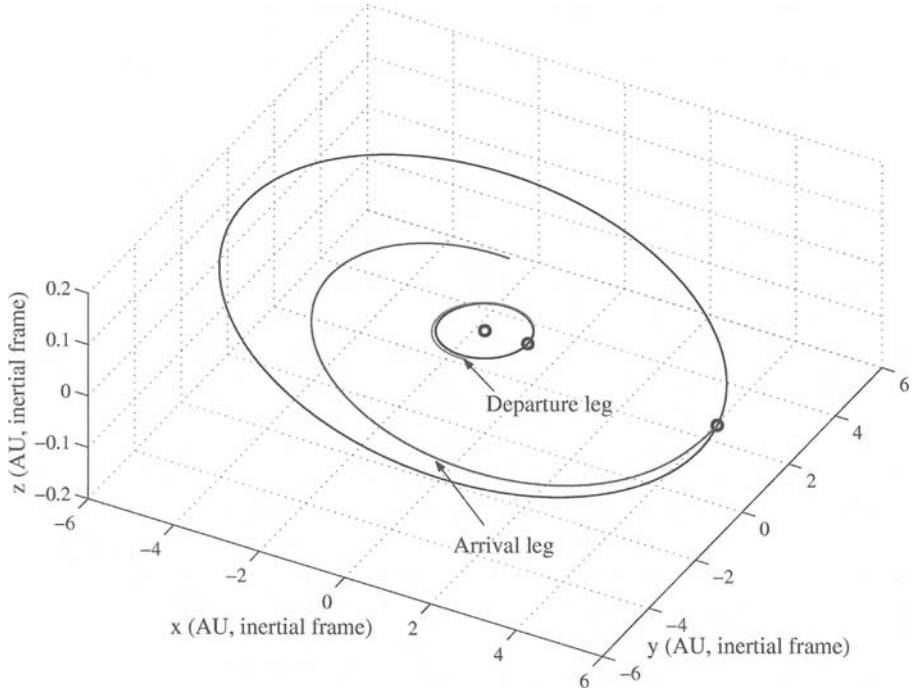

FIG. 7. Departure and Arrival Legs in the Sun-Centered Inertial Frame.

where the four terms are explained as follows:

- Δv_S: cost required to inject the spacecraft in a transit orbit inside the unstable manifold starting from a r_S circular orbit around the departure planet;
- Δv_1: cost of the first deep space maneuver necessary to "jump" from the unstable trajectory to the conic arc;
- Δv_2: cost of the second deep space maneuver necessary to inject the spacecraft on the captured transit leg;
- Δv_E: cost required to place the spacecraft in a r_E circular orbit around the arrival planet.

As discussed in the previous section, the two transit orbits are generated by perturbing two points defined on the Poincaré section of the manifolds and their propagation stops when the closest approach with the planet is reached. Hence the two radii r_S and r_E depend on the set of chosen variables. If the cost for the analogous Hohmann transfer, linking the same starting and arriving circular orbits, is defined as

$$\Delta v_H = \Delta v_H(r_S, r_E) = \Delta v_H(r_S(\mathbf{x}), r_E(\mathbf{x})) = \Delta v_H(\mathbf{x}) \tag{23}$$

then the objective function used for the optimization of the transfer is

$$f(\mathbf{x}) = \Delta v(\mathbf{x}) - \Delta v_H(\mathbf{x}) \tag{24}$$

In (24) both the total cost of the patched conic-manifold transfer and the cost for the analogous Hohmann transfer are functions of the state variable $\mathbf{x}$. Therefore the value $\mathbf{x} = \mathbf{x}^*$ which makes $f(\mathbf{x}^*)$ negative is expected to correspond to the optimal altitude for the arrival and departure orbits.

Hybrid Optimization of the Transfer

The problem stated in the previous section is solved splitting the optimization into two steps:

- a first global search, implemented with an evolutionary algorithm (EA), explores the search domain and provides a good initial solution;
- a local optimization, employing a sequential quadratic programming (SQP) algorithm, is used to further refine the solution found by the EA.

The selection of this sequence is due to the nature of the present problem: since the SQP algorithm is a gradient based method, it requires an initial condition to start the search; if this condition lies inside the basin of attraction of the global minimum, the SQP will converge to it. Since it is very difficult to provide a good first guess solution for the problem stated above, due to the complex relations among the objective function $f(\mathbf{x})$, the state variable $\mathbf{x}$ and the corresponding trajectory, the EA, by its extended preliminary search in the whole domain, is able to assure a good first guess solution to the SQP. The integer n_f is used to indicate the total number of function evaluations and it is equal to the sum $n_f = n_f^{EA} + n_f^{SQP}$ where n_f^{EA} and n_f^{SQP} are respectively the evaluations required to the EA and to the SQP. Figure 8 illustrates the typical convergence profile of the objective function versus the total number evaluations. The solid line represents the EA convergence history while the dashed line, leading to the final value (the star on the bottom-right), is the SQP step.

Study Cases

In this section the patched conic-manifold approach, described in the previous section, is applied to the design of some representative transfers among inner planets. The cases considered here are the transfers from Earth to Venus and from Earth to Mars. The results are compared in terms of total Δv and Δt to the corresponding

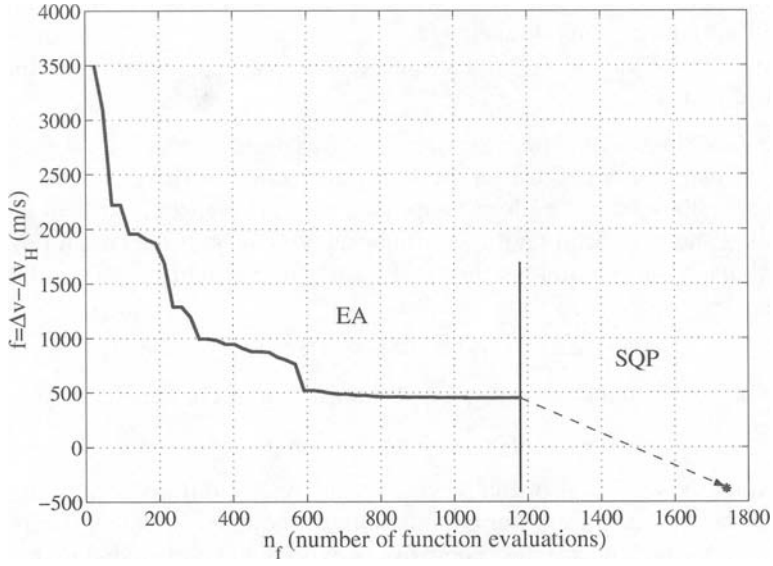

FIG. 8. A Typical Convergence History of the Objective Function f Versus n_f.

classical bicircular Hohmann transfers between the same departure and arrival circular orbits, with radius r_S and r_E, around the two planets considered. In particular, as stated in equation (24), the solutions are compared in terms of the objective function $f = \Delta v - \Delta v_H$ where the total cost Δv takes into account the two maneuvers around the planets (Δv_S and Δv_E) and the two additional deep space maneuvers (Δv_1 and Δv_2) necessary to perform the injection from the manifold to the conic arc and vice versa. The search has been performed over a wide launch window starting in 2010 and ending in 2020 and a set of three representative solutions are presented for each case showing the effectiveness of the developed algorithm.

Earth-Venus Transfer

The solutions found for the Earth-Venus case, represented in Table 2, show that the objective function f is negative; this means that these transfers are cheaper than the Hohmann solutions. This result confirms that the patched conic-manifold trajectories, as expected, are more energetically efficient than the corresponding patched conics.

Solution 2, the best found in this study, has a total cost equal to $\Delta v = 3843$ m/s while the analogous Hohmann transfer costs $\Delta v_H = 4395$ m/s. The first maneuver ($\Delta v_S = 202$ m/s) injects the spacecraft in a transit orbit inside the (W^U_{L1po}) of the Sun-Earth system departing from a high altitude circular orbit around the Earth. The second burn ($\Delta v_1 = 2362$ m/s) is used to lower the perihelion of the conic arc while the third maneuver ($\Delta v_2 = 1310$ m/s) places the spacecraft inside the (W^S_{L2po}) of the Sun-Venus system. Finally, the fourth maneuver ($\Delta v_E = 150$ m/s) is used to stabilize the spacecraft in a high altitude circular orbit around Venus. This solution takes 766 days to reach Venus, while the time of flight for a Hohmann transfer is 145 days long. Solutions 1 and 3 have a total cost equal to $\Delta v = 4208$ m/s ($\Delta v_S = 368$ m/s), ($\Delta v_1 = 2034$ m/s), ($\Delta v_2 = 1752$ m/s) ($\Delta v_E = 52$ m/s), and $\Delta v = 4051$ m/s ($\Delta v_S = 440$ m/s), ($\Delta v_1 = 472$ m/s), ($\Delta v_2 = 3014$ m/s), ($\Delta v_E = 124$ m/s) therefore, since they refer to different parking orbits, they turn out to be again cheaper than the corresponding Hohmann solutions. Figure 9 shows a typical portrait of the arrival transit orbit circularized around Venus. Figure 10 shows a detail of the arrival transit orbits associated to Solutions 1 and 2 in a neighborhood of the L_2 point. In this frame the problem is autonomous and the algorithm selects two close solutions characterized by different departure epochs. Figure 11 illustrates a typical interplanetary trajectory associated to an Earth-Venus transfer. The algorithm finds similar transit orbits for any simulation because, as the above results demonstrate, the objective function (24) is influenced mostly by the two deep space maneuvers characterized by the configuration of the planets. Hence the transit orbits need only to be slightly adjusted to provide the best initial conditions for the Lambert's arc depending on the starting epoch.

TABLE 2. Solutions for the Earth-Venus Transfer

T_S (MJD)	f (m/s)	Δv (m/s)	Δv_H (m/s)	Δt (days)	r_s (km)	r_E (km)
4741	−47	4208	4255	571	207700	334530
5813	−552	3843	4395	766	525590	384380
6561	−156	4051	4207	494	173520	294710

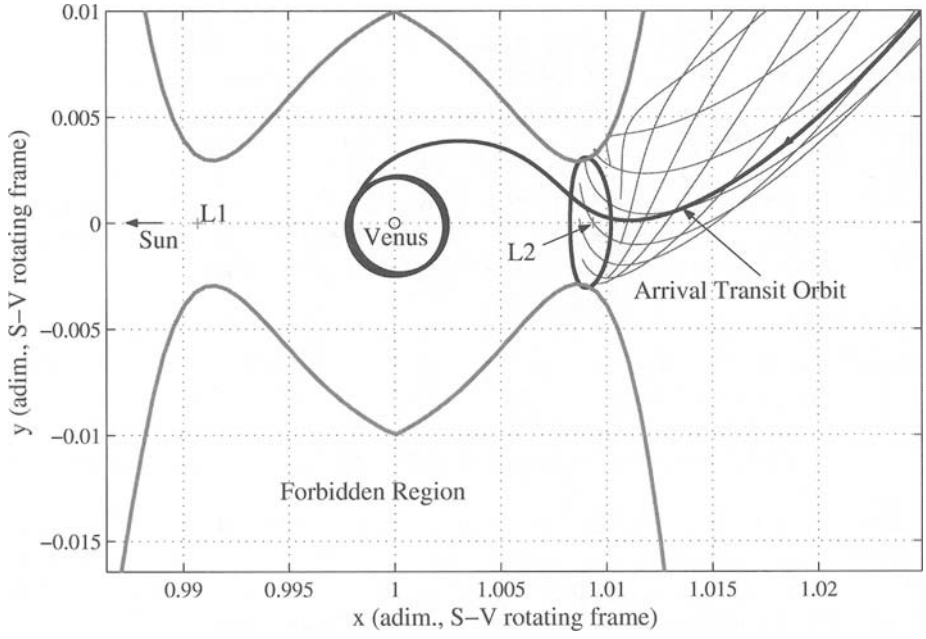

FIG. 9. Arrival Leg and Final Circular Orbit Around Venus (Sun-Venus Rotating Frame).

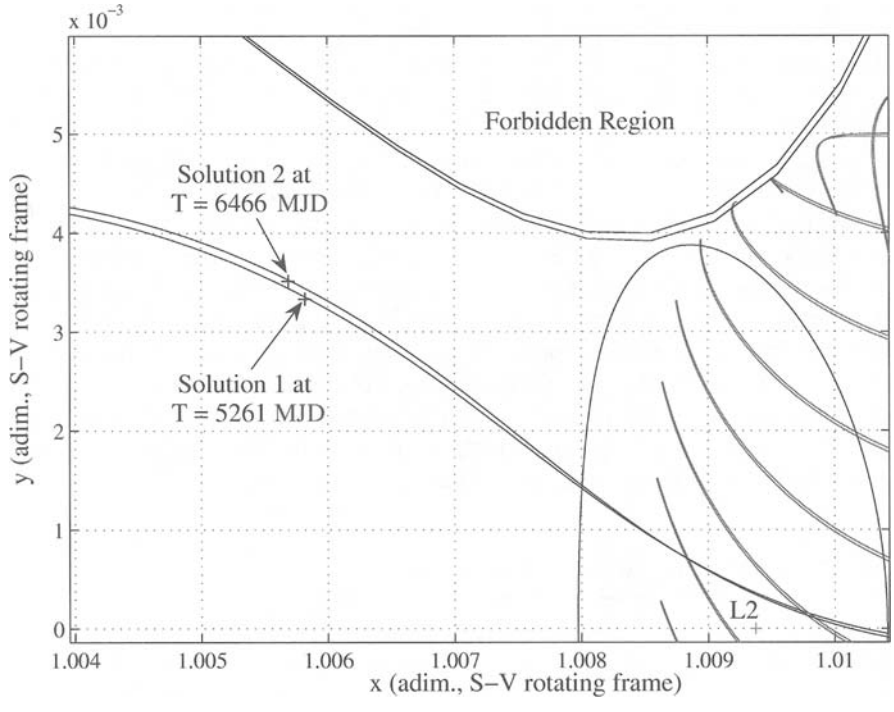

FIG. 10. Transit Orbits Corresponding to Solutions 1 and 2.

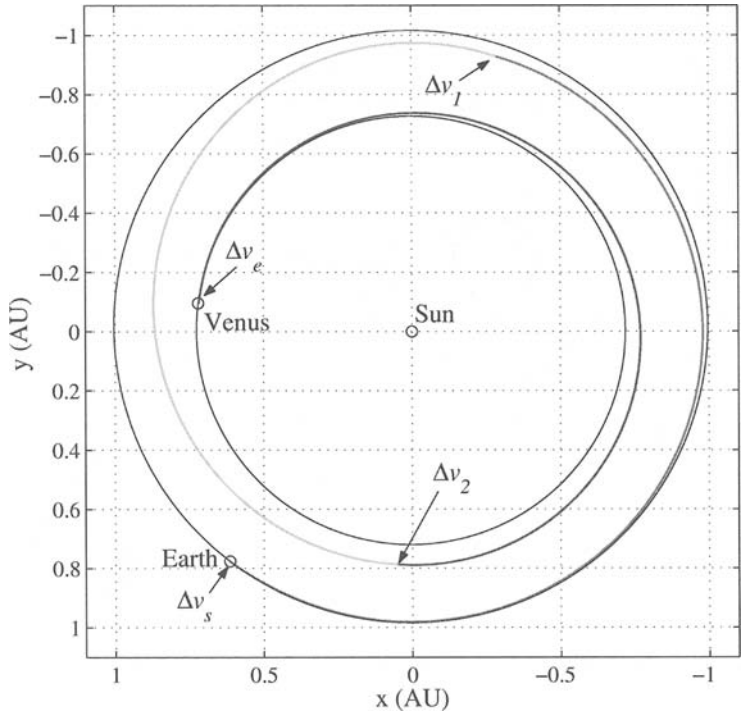

FIG. 11. Interplanetary Patched Conic-Manifold Transfer Trajectory to Venus.

It must be pointed out that these results correspond to 3-D trajectories and so the change of the inclination has been also taken into account in the total cost. The results found in this section are expected to be quite accurate if compared to equivalent transfers computed in a full four-body problem; this is due to the small value of the orbital eccentricity of both Earth and Venus, $e = 0.006$ and $e = 0.016$ respectively, that makes the circular R3BP a good model to derive these low energy transfers.

Earth-Mars Transfer

The solutions for the Earth-Mars transfer are summarized in Table 3. Also in this case these results present negative values of the objective function making these trajectories cheaper than the Hohmann transfers. Solution 1 presents a $\Delta v = 3755$ m/s and a time of flight equal to 999 days; the corresponding Hohmann transfer costs $\Delta v_H = 4436$ m/s and is 246 days long. Solutions 2 and 3 allow savings of 588 m/s

TABLE 3. Solutions for the Earth-Mars Multi-Burn Transfer

T_S (MJD)	f (m/s)	Δv (m/s)	Δv_H (m/s)	Δt (days)	r_s (km)	r_E (km)
3861	−681	3755	4436	999	185940	142820
4169	−588	4105	4693	707	410270	317040
7203	−429	3967	4396	910	165200	123760

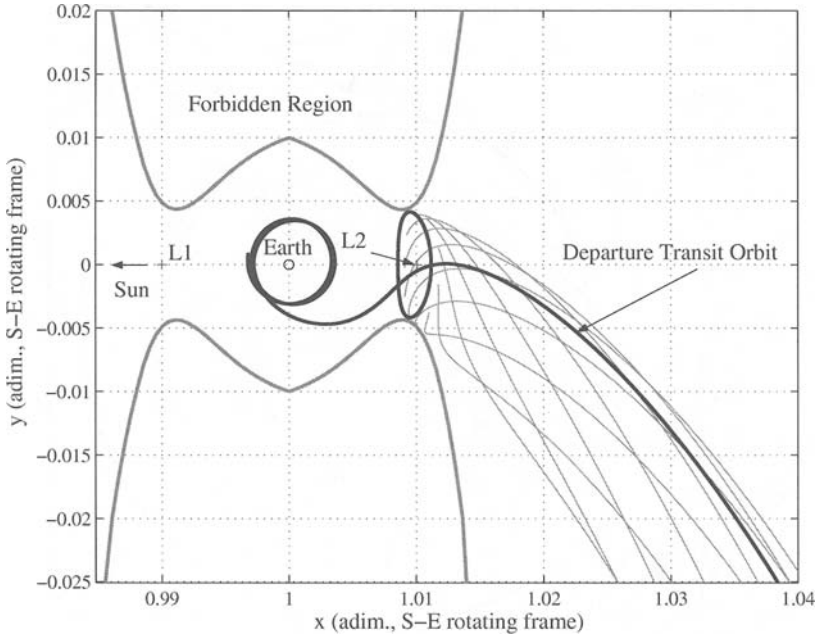

FIG. 12. Departure Transit Orbit, Escaping from the Earth, for a Transfer to Mars.

and 429 m/s because they cost $\Delta v = 4105$ m/s and $\Delta v = 3967$ m/s while the Hohmann solutions need $\Delta v_H = 4693$ m/s and $\Delta v_H = 4396$ m/s.

Figure 12 shows the circular orbit around the Earth and the transit orbit into the unstable manifold tube; Fig. 13 illustrates the typical interplanetary path for the Earth-Mars transfer. The three legs have here the same meaning as in the Earth-Venus

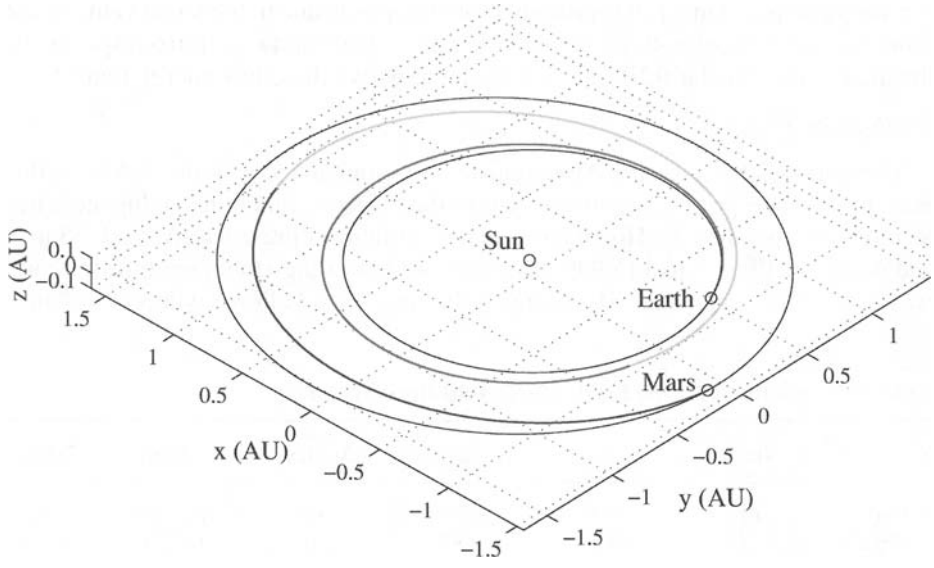

FIG. 13. Interplanetary Earth-Mars Patched Conic-Manifold Transfer Trajectory.

case with the only difference that this time the departure occurs from the exterior tube ($W^U_{L_{2po}}$) of the Sun-Earth system) and the arrival leg is close to Mars' interior equilibrium point ($W^S_{L_{1po}}$ of the Sun-Mars system).

The orbital eccentricity of Mars is $e = 0.093$, thus a small error is expected in the description of the arrival leg since this time the circular R3BP is not adequate to describe the real Sun-Mars-Spacecraft dynamics as in the former case.

The achieved results show that the use of the transit orbits, in the R3BP, leads to a substantial saving in Δv for interplanetary travels toward Venus and Mars. Such a saving is paid in terms of time of transfer which is on average one and half year longer, for a transfer to Venus, and more than two years long, for a transfer to Mars. This is due to the slow dynamics, in the neighborhood of the libration points, governing the transit orbits. Moreover, the method described above, through the equation (18), selects two transit orbits shadowing the asymptotic paths associated to the periodic orbits. This means that, among all the transit orbits, the ones used to generate the transfers are dynamically close to the asymptotic orbits and thus they lead to a slow approach and departure from the planet.

Conclusions

This paper describes a method that expands the technique of using invariant manifolds with systems where the physical parameters do not allow any intersection between two manifolds in the configuration space. The resulting low energy trajectories can be used for interplanetary transfers among inner planets.

The results found for both transfers to Venus and to Mars show that a saving in the propellant mass fraction is possible by exploiting the three-body dynamics in the neighborhood of the collinear libration points L_1 and L_2 of the generic Sun-planet-spacecraft problem. The cheapest solution found for the Earth-Venus case allows savings up to 12% in total Δv if compared with the analogous Hohmann transfer. Nevertheless, the shortest solution has a time of flight that is more than 300% of the Hohmann one. If the patched conic-manifold method is applied to design an Earth-Mars transfer, up to 15% of the total Δv can be saved, but the time of flight increases. The shortest solution, indeed, is 280% longer than the corresponding Hohmann transfer.

Thus, the main drawback of such transfers is the high time of flight. Even if the cost reduces the time of flight increases up to three times compared to the Hohmann transfer. Therefore these trajectories are suitable for missions, as the ones cited above, where the payload mass must be maximized without any particular constraint on the time of transfer.

Since the full trajectories computed in this work have been obtained by patching arcs obtained with different dynamics, the whole interplanetary paths need to be verified in a more refined model describing the real n-body dynamics of the solar system.

A final remark concerns the starting and arrival circular orbits that the developed method, by itself, selects. The results summarized in Tables 2 and 3 show that very high altitude circular orbits can be linked with the patched conic-manifold method. This outcome appears also when just the total cost (Δv) is optimized instead of the fitness function (24). This is a consequence of the intrinsic nature of the problem: in order to bound the energy of the transit orbits, small amplitude periodic orbits are selected to generate the invariant manifolds tubes. It is well known that below certain amplitudes of the periodic orbits such manifolds do not approach the smallest

primary [4], thus a direct link between a low energy transit orbit and a low altitude orbit around a planet is forbidden *a priori*. If the energy level increases, high amplitude orbits can be obtained with their manifolds coming close to the planets. Unfortunately, in these cases the benefits are lost and an interplanetary transfer computed with the patched conic-manifold method is not convenient. A further development, currently under investigation, concerns the use of elliptical orbits, instead of the circular, to link a low altitude point close to the planet and a transit orbit.

References

[1] JEHN, R., CAMPAGNOLA, S., GARCIA, Y., and KEMBLE, S. "Low-Thrust Approach and Gravitational Capture at Mercury," 18th Symposium on Space Flight Dynamics, Munich, Germany, October 11–15, 2004.

[2] BELBRUNO, E. A. and MILLER, J. K. "Sun-Perturbated Earth-to-Moon Transfers with Ballistic Capture," *Journal of Guidance, Control and Dynamics,* Vol. 16, No. 3, July-August 1993, pp. 770–775.

[3] LLIBRE, J., MARTÌNEZ, R., and SIMÒ, C. "Transversality of the Invariant Manifolds associated to the Periodic Orbits near L_2 in the Restricted Three-Body Problem," *Journal of Differential Equations,* No. 58, 1985, pp. 104–156.

[4] HOWELL, K. C., BARDEN, B. T., and LO, M. W. "Application of Dynamical System Theory to Trajectory Design for a Libration Point Mission," *The Journal of the Astronautical Sciences,* Vol. 45, No. 2, April-June 1997, pp. 161–178.

[5] KOON, W. S., LO, M. W., MARSDEN, J. E., and ROSS, S. D. "Heteroclinic Connections Between Periodic Orbits and Resonance Transition in Celestial Mechanics," *Chaos,* Vol. 10, No. 2, June 2000, pp. 427–469.

[6] KOON, W. S., LO, M. W., MARSDEN, J. E., and ROSS, S. D. "Low Energy Transfers to the Moon," *Celestial Mechanics and Dynamical Astronomy,* Vol. 81, No. 1, September 2001, pp. 63–73.

[7] KOON, W. S., LO, M. W., MARSDEN, J. E., and ROSS, S. D. "Constructing a Low Energy Transfer Between Jovian Moons," *Contemporary Mathematics,* Vol. 292, February 2002, pp. 129–145.

[8] SZEBEHELY, V. *Theory of Orbits: the Restricted Problem of Three Bodies,* Academic Press Inc., New York, 1967.

[9] GÒMEZ, G. and MONDELO, J. M. The "Dynamics Around the Collinear Equilibrium Points of the RTBP," *Physica D,* Vol. 157, October 2001, pp. 283–321.

[10] JORBA, A. and MASDEMONT, J. "Dynamics in the Center Manifold of the Collinear Points of the Restricted Three Body Problem," *Physica D,* Vol. 132, July 1999, pp. 189–213.

[11] YAMATO, H. and SPENCER, D. "Transit-Orbit Search for Planar Restricted Three-Body Problem with Perturbations," *Journal of Guidance, Control and Dynamics,* Vol. 27, December 2004, pp. 1035–1045.